1 The Feasibility of Reconstructing Hydroclimate over West Africa using Tree-Ring Chronologies

2 in the Mediterranean Region

3

4 Boniface O. Fosu[1], Edward R. Cook[2], Michela Biasutti[2], Brendan M. Buckley[2], Sharon E.

5 Nicholson[3]

6

7 [1]Department of Geosciences, Mississippi State University, Mississippi State, MS, USA.

8 [2]Lamont-Doherty Earth Observatory of Columbia University, Palisades, NY, USA.

9 [3]Earth, Ocean and Atmospheric Sciences, Florida State University, Tallahassee, FL, USA.

10

11 Correspondence

12 Boniface O. Fosu, Department of Geosciences, Mississippi State University, MS State, MS, USA.

13 Email: boniface.fosu@msstate.edu

14

15 **Abstract**

16 Dendrochronology in West Africa has not yet been developed despite encouraging reports

17 suggesting the potential for long tree-ring reconstructions of hydroclimate in the tropics. This

18 paper shows that even in the absence of local tree chronologies, it is possible to reconstruct

19 the hydroclimate of a region using remote tree-rings. We present the West Sub-Saharan

20 Drought Atlas (WSDA), a new paleoclimatic reconstruction of West African hydroclimate

21 based on tree-ring chronologies from the Mediterranean Region, made possible by the

22 teleconnected climate relationship between the West African Monsoon and Mediterranean Sea

surface temperatures. The WSDA is a one-half degree gridded reconstruction of summer Palmer Drought Severity indices from 1500–2018 CE, produced using ensemble point-by-point regression. Calibration and verification statistics of the WSDA indicate that it has significant skill over most of its domain. The three leading modes of hydroclimate variability in West Africa are accurately reproduced by the WSDA, demonstrating strong skill compared to regional instrumental precipitation and drought indices. The WSDA can be used to study the hydroclimate of West Africa outside the limit of the longest observed record and for integration and comparison with other proxy and archaeological data. It is also an essential first step toward developing and using local tree-ring chronologies to reconstruct West Africa's hydroclimate.

Keywords

West Africa, Mediterranean, Hydroclimate, Tree-ring network, Teleconnection, Drought Atlas

1.0 Introduction

Recent hydroclimatic changes in West Africa have visibly adverse socioeconomic ramifications (Turco et al 2015). For instance, in 2015, severe drought limited water availability in the Volta River Basin, an essential source of water distribution and economic activity in West Africa. Consequently, electricity generation by several dams within the basin came to a halt, including the Akosombo Dam, the single largest electricity source in Ghana, crippling the country's economy and threatening the basic livelihood of many of its already impoverished communities.

45   Policies premised on leveraging science and technology hold the greatest promise to mitigating

46   such climate driven economic impacts, but their formulation is limited by the lack of important

47   information and considerable uncertainty in the projections of hydroclimatic variability in

48   West Africa (Challinor et al 2007, Biasutti 2009, Roudier et al 2011, Biasutti 2013).

49   Long observational records for key climatic variables against which to evaluate the

50   performance of climate models, the primary tools for climate projections, are rare in West

51   Africa. In fact, only during the 1930's did synoptic observation stations become generally

52   established in the sub-region and these remain sparse even today (Tarhule and Hughes 2002).

53   The instrumental record is thus often too short to give an adequate account of the range of

54   possible behavior of the region's climate and is not enough to vet model performances in

55   reproducing them. In addition, lack of long observational records limits our ability to

56   accurately attribute the relative contributions of human influences versus natural variability

57   to recent hydroclimatic changes and provides an unreliable baseline for deriving

58   observationally constrained estimates of future climate projections based on a past climate

59   regime. Ultimately, this precludes a proper assessment.

60   In the absence of ample instrumental records, dendrochronological methods of climate

61   reconstruction have yielded unique insights into the natural variability of Earth's climate

62   system (Cook and Kairiukstis 1990, Cook et al 2010, Buckley et al 2010, Anchukaitis 2017),

63   thus allowing us to test model performances outside the limit of the longest observed record.

64   Due to their strong response to environmental changes, trees are particularly well suited for

65   studying hydroclimate variability (St. George 2014, St. George and Ault 2014), although the

66   specific monthly or seasonal climate response can vary across regions and continents (St.

67   George et al 2010, Touchan et al 2014). Trees provide annually resolved information on past

68   climate variability and can be dated to the exact calendar year, thus enabling quantitative and

69   precise calibration and verification. Despite inherent uncertainties, proxy data, including tree

70   rings can be used in conjunction with instrumental records to reduce uncertainty in

71   hydroclimatic projections (Henderson et al 2009, Haywood et al 2019).

72   The potential for dendrochronology in West Africa has not yet been developed,

73   notwithstanding the vital role it often plays in our understanding of past hydroclimate

74   variability and future climate projections. To date, paleolimnological investigations of the

75   Kajemarum oasis in the Manga Grassland of northeastern Nigeria have furnished much of the

76   information on Holocene climate for West Africa (Salzmann 1996, Waller and Salzmann 1999,

77   Street-Perrot et al 2000).

78   In this study, we show that even in the absence of local tree chronologies, it is possible to

79   reconstruct the hydroclimate of a region using remote tree-ring growth. We present a Palmer

80   Drought Severity Index (PDSI) reconstruction as a proxy for the hydroclimate over West Africa

81   based on tree-ring chronologies from the Mediterranean region. This is made possible by a

82   strong teleconnection signal between the Mediterranean region and West Africa. Rowell

83   (2003) first demonstrated the positive influence of Mediterranean Sea surface temperatures

84   (SST) anomalies on West African Monsoon (WAM) precipitation through northerly moisture

85   advection from the Mediterranean toward the Sahel. Since then, a number of studies including

86   Jung et al 2006, Peyrille and Lafore 2007, and Diatta et al 2020 have been dedicated to the

87   WAM-Mediterranean interaction and the existence of this teleconnection is now widely
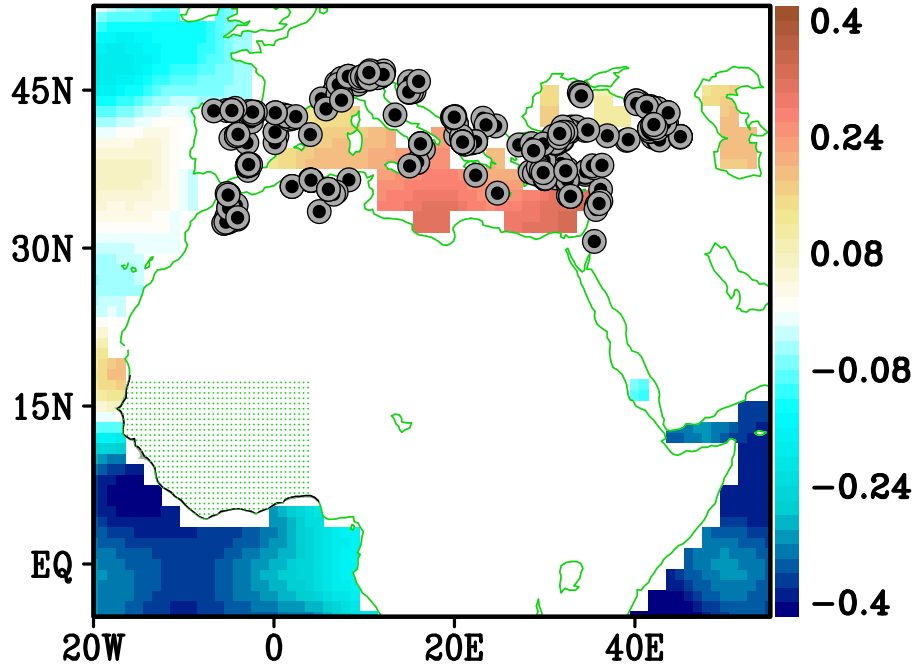
88   accepted.

89

Figure 1: Geographic context for the study. Shaded black circles with gray outlines represent the 333 sites of the tree-ring chronologies utilized in reconstructed scPDSI over West Africa (i.e., WSDA). The one-half degree grid points (i.e., green dots) represent the WSDA grid. Shading outside land areas represent the summer (JJA) correlation between SST and the time series of EOF1 of instrumental scPDSI over West Africa, from 1901-2020.

Our results are encapsulated in the novel West Sub-Saharan Drought Atlas (WSDA, figure 1), an annually resolved spatial reconstruction of West Africa's hydroclimate over the past five hundred years. The WSDA can be used to assess the performance of climate models and for integration and comparison with other proxy, historical, and archaeological data. It is also an important first step toward the goal of developing and using local tree-ring chronologies to reconstruct West Africa's hydroclimate.

2.0 Data and Methodology

2.1 Tree-ring Network and Reconstruction Method

The tree-ring network we used for the WSDA reconstruction is based on the Mediterranean portion of the Old-World Drought Atlas tree-ring network (Cook et al 2015). It is comprised of 333 tree-ring chronologies and its spatial distribution is shown in figure 1. All chronologies begin on or before 1798 and end no earlier than 1990. We used this network because of its previous success in reconstructing past drought over the Mediterranean region and its clear association with the Mediterranean teleconnections that influence West Africa rainfall.

The method of reconstruction we used is the Point-by-Point Regression (PPR) method (Cook et al 1999) and its extension to ensemble PPR (EPPR) as described most recently in Cook et al (2020). PPR was specifically developed for the reconstruction of hydroclimate variability from tree rings, but it originally relied on relatively local tree-ring chronologies to reconstruct local hydroclimate (Cook et al 1999). This limitation was relaxed through the use of multiple search radii for locating tree-ring chronologies in more remote locations to reconstruct hydroclimate at each grid point and a novel correlation-weighted method for generating the principal component regression models used for reconstruction (Cook et al 2010a, 2020). This resulted in an ensemble of reconstructions at each grid point (hence EPPR) that could be evaluated for skill.

The tree-ring chronologies used for reconstruction have a common end year of 1990 because of the widely varying years in which the trees were sampled but lose one year (1990) due to the inclusion of a lagged tree-ring variable in the model (Cook et al 1999). For this reason,

123   the calibration period chosen for developing the reconstructions was set to 1951–1989. This

124   period includes the highest number of rainfall stations used for calculating the self-calibrating

125   Palmer Drought Severity Index (scPDSI) over West Africa (figure 2 in Nicholson et al 2018)

126   and therefore ought to be the highest quality period for calibrating each EPPR model. Of the

127   remaining pre-1951 scPDSI data, only the 1920–1950 period was used for model validation

128   because of the sharply declining number of rainfall stations over West Africa in the early 20th

129   Century (figure 2 in Nicholson et al 2018).

130   The WSDA reconstructions cover the period 1500-2018 CE. Each grid point reconstruction has

131   been scaled to recover lost variance due to regression (proportional to $1-R^2$). This enabled

132   each reconstruction to be updated from 1990 to 2018 with instrumental data.

133   2.2 Calibration and Verification Statistics

134   We provide five rigorous calibration and verification statistics that are typically used for

135   assessing the quality of dendroclimatic reconstructions (e.g., Michaelsen 1987, Meko 1997,

136   Cook et al 1999). They include the calibration period coefficient of determination or R^2

137   (CRSQ) and cross-validation reduction of error (CVRE). The latter is a 'leave-one-out'

138   procedure analogous to R^2 based on Allen's PRESS statistic (Allen 1971) and its R^2 equivalent

139   (Quan 1988) and is a more conservative measure of explained variance than CRSQ. In

140   extremely weak calibration cases CVRE can actually go negative, which is a clear indication of

141   no calibration skill.

142   The validation period statistics are the square of the Pearson correlation (VRSQ, sign of the

143   correlation applied), the reduction of error statistic (VRE), and the coefficient of efficiency

144 (VCE), and these can be interpreted as expressions of shared variance between the actual data

145 and the tree ring estimates. Negative values indicate no reconstruction skill as measured. The

146 formulae of these statistics require that VRSQ is greater than or equal to VRE, which in turn is

147 greater than or equal to VCE when calculated from the same data, thus making VCE the

148 hardest validation statistic to pass. No theoretical significance tests are available for the VRE

149 and VCE. Simply, values greater than zero indicate that the reconstruction has skill in excess

150 of the calibration or verification period climatology of the instrumental data. In addition to

151 these validation metrics, the root mean square error (RMSE) statistic is provided as a simple

152 estimate of uncertainty. For a full explanation of these statistics, the reader is referred to Cook

153 et al (1999).

154 2.3 Hydroclimatic and SST Datasets

155 The instrumental hydroclimate data used for statistical calibration and validation in this study

156 is the widely used self-calibrating Palmer Drought Severity Index (scPDSI; Wells et al 2004,

157 van der Schrier et al 2013), specifically the CRU TS 4.03 dataset that covers the period 1901-

158 2018 (Barichivich et al 2018). It is calculated from the University of East Anglia's Climatic

159 Research Unit's instrumental temperature and precipitation dataset, available on a 0.5°

160 resolution from 1901 to the present. From these monthly data we reconstructed the summer

161 (June-August) average scPDSI over West Africa. This matches the season reconstructed for the

162 OWDA and also coincides with the summer rainfall season over the WSDA domain.

163 We also used the Joint Institute for the Study of the Atmosphere and Ocean (JISAO) Sahel

164 precipitation index which spans 1901 to present, derived from the 0.25° resolution Deutscher

165 Wetterdienst Global Precipitation Climatology Centre monthly precipitation dataset and the

166   Sahel rainfall time series from Nicholson et al (2018), which is based on 602 rain gauge

167   records of variable length extending from 1854 to 2014. A comparative series for the Gulf of

168   Guinea region to the south is also utilized. Together, the latter two rainfall indices from

169   Nicholson et al (2018), hereafter referred to as NRI, collectively provide insight into the long-

170   term variability of the West African monsoon.

171   Apart from these meteorological datasets, we make use of the Hadley Center Sea Ice and Sea

172   Surface Temperature dataset (HadISST, Rayner et al 2003), which is analyzed in concert with

173   the aforementioned instrumental scPDSI to deduce the connection between West African

174   hydroclimate and Mediterranean SST.

175   2.4 EOF Analysis

176   The primary goal of Empirical orthogonal function (EOF) analysis is to simplify a given space-

177   time dataset by extracting the smallest set of independent modes of variability that can

178   adequately describe it (e.g., Lorenz 1956, LaMarche and Fritts 1971). Standard EOFs are

179   found by computing the eigenvalues and eigenvectors of the anomaly covariance matrix of a

180   field. The eigenvalues provide a measure of the percent variance explained by the

181   corresponding mode, the latter are orthogonal to each other depending on the time period

182   being used. The time series (aka principal component or PC) of each mode is determined by

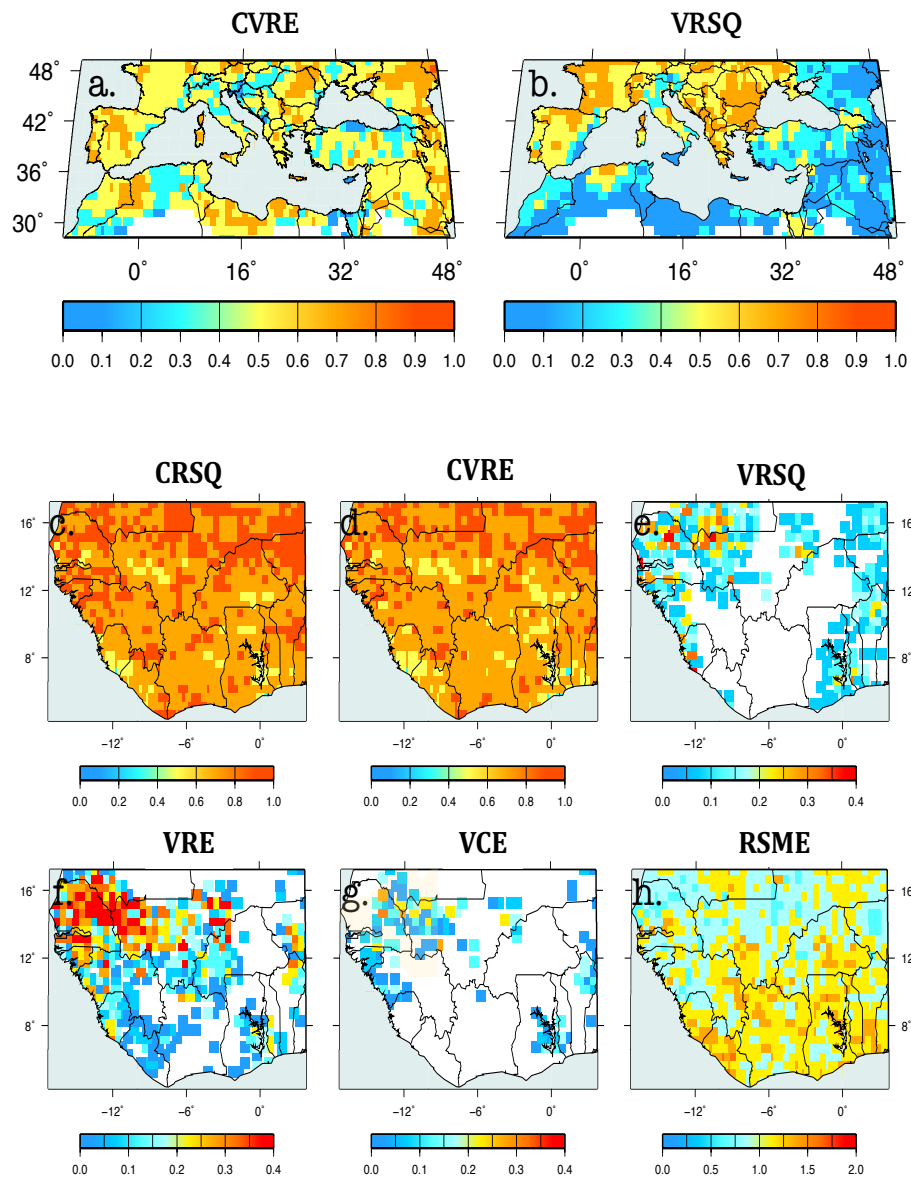183   projecting the derived eigenvectors onto the spatially weighted anomalies.

184   Here, we use EOFs to identify the coherent patterns in the reconstructed hydroclimate over

185   West Africa and the Mediterranean Region and evaluate them against the instrumental scPDSI

186   and precipitation datasets. Typically, the first few modes contain the most variance as well as

187   physically interpretable patterns when it comes to atmospheric and hydroclimatic processes,

188   so in this paper, we focus on the first three EOFs. All analyses are based on the Boreal summer

189   months of June, July, and August (i.e., JJA). Also, datasets are normalized before use in order

190   to prevent areas of maximum variance from dominance and facilitate comparison.

191   **3. Results and Discussion**

192   Figure 1 shows the locations of the tree-ring chronologies used for reconstructing the WSDA,

193   the WSDA domain limits, and how the first principal component (PC1) of instrumental scPDSI

194   over the WSDA is correlated to SSTs in the Mediterranean from 1901-2020. The strength and

195   pattern of the correlations are consistent with the known teleconnection between the two

196   regions, which is primarily characterized by the WAM response to thermal Mediterranean

197   forcing. When the Mediterranean is warmer than normal, it reinforces the northward

198   migration of the monsoon system and surface convergence in the vicinity of the intertropical

199   convergence zone (ITCZ) through stronger moist convection south of the Sahara. The

200   increased moisture convergence feeds the convective activity leading to increased precipitation

201   (Rowell 2003, Gaetani et al 2010, Fontaine et al 2010). On the other hand, the alternate effect

202   of WAM dynamics on Mediterranean climate is not as clearly understood, although a few

203   studies including Rodwell and Hoskins (2001) argue that the Rossby wave response to West

10

204 African monsoonal heating, interacting with midlatitude westerlies, does impact

205 Mediterranean climate by producing a strong region of adiabatic descent there.

206

Figure 2: Reconstruction drought calibration and verification statistics. (a-b) Mediterranean
Region cross-validation RSQ (CVRE) and validation period RSQ (VRSQ). (c-d) WSDA
calibration period RSQ (CRSQ) and cross-validation RSQ (CVRE). (e-g) WSDA validation RSQ

210 (VRSQ), validation period reduction of error (VRE) and validation period coefficient of

211 Efficiency (VCE). Unlike CRSQ, which can never be negative, CVRE, VRSQ (by retaining the

212 sign of r after squaring), VRE and VCE can have negative values, indicating that there is no

213 skill in the estimates. All but RSME are in units of fractional explained variance. RSQ is $R^{2.}$

214

215 Calibration and verification results over the Mediterranean and WSDA grids are presented in

216 figure 2, providing an avenue to measure the quality of reconstructions from the local

217 chronologies and a benchmark against which to evaluate the reconstruction of the remote

218 hydroclimate in West Africa. Most of the grid points show reasonably robust calibrations

219 (figure 2(a)), with a validation skill map that exhibits a diagonal split between high skill in

220 the northwest and relatively low skill in the southeast (figure 2(b)). The latter may be caused

221 in part by a decline in the number of rainfall records contributing to the scPDSI estimates

222 especially over Turkey and the Middle East, thus resulting in reduced instrumental data quality

223 especially before 1930. Recall that the Mediterranean tree ring chronologies utilized in this

224 study were previously used to build the Old World Drought Atlas (OWDA) as presented in

225 Cook et al. 2015, which elaborates further on the quality of instrumental and proxy

226 reconstructions in the region.

227 Over the West Africa grid, we present four additional validation metrics, given that the WSDA

228 is the main focus of this paper. Much like the Mediterranean, the entire WSDA grid calibrates

229 well (figures 2(c) and (d)), with weaker but useful validations indicated by the positive VRSQ,

230 VRE and VCE, scattered across the domain (figures 2(e) – (g)). Judging by the VCE, which is

231 the hardest metric to pass, it is clear that the most consistent and reliable validation occurs

232   along the main river systems of two of the three biggest watersheds in West Africa (figure S1).

233   Within the Volta River Basin to the east, the best grids show up along the Volta River in Ghana.

234   In the west, they appear along the Sénégal River within the Senegal River Basin (figure 2(g)).

235   The RMSE's in figure 2(h) provide more insight into the magnitude of the total errors of the

236   WSDA reconstructions, both bias and variance. In congruence with the other validation

237   metrics, the lowest reconstruction skill is largely found over the central part of the region.

238   One possible reason for the low skill validations is the poor quality of observations particularly

239   before 1951, when fewer stations are available and most grid point interpolations are relaxed

240   towards the climatology as available stations diminish. The relatively strong validity of the

241   reconstruction over the Northwestern Mediterranean and within specific river basins is also

242   not surprising. Historically, humans have settled close to water bodies and food sources

243   because of commerce and trade and would provide an economic incentive to take

244   hydroclimatic measurements there. Any long systematically measured data within the WSDA

245   grid implicitly augurs well for its validation.

246   Considering the limitations with historical data at the grid point scale, we proceeded to

247   evaluate the utility of the WSDA on a regional scale by comparing EOFs of the instrumental

248   and reconstructed summer scPDSI in figure 3. EOF1 of the instrumental scPDSI (figure 3(a))

249   explains 44% of the total variance and exhibits a monopole mode of variability or anomalous

250   conditions of the same sign throughout the region. EOF2 explains 10% of the variance and is

251   characterized by a meridional dipole pattern of variability, which represents the well-known

252   dipole of hydrological conditions over the Sahel region and the Gulf of Guinea (e.g., Nicholson

253   et al 2013). So, wet conditions in the Sahel are opposed by dry conditions on the Guinea Coast,

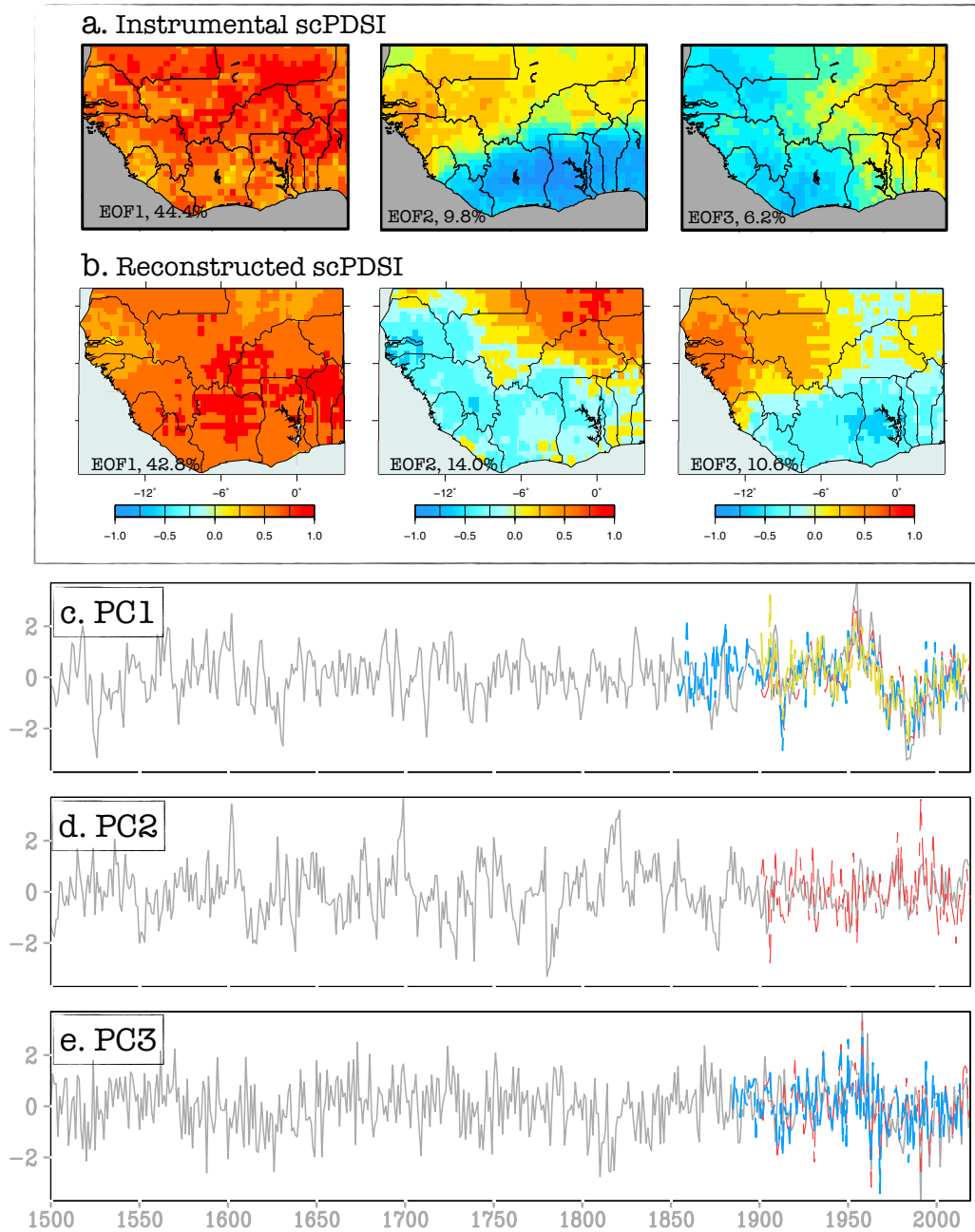254   and vice versa. Nicholson and Grist (2001) describe these two modes as so fundamental that

255

Figure 3: EOF patterns of (a) instrumental scPDSI over West Africa (spanning 1901-2020)

257   and (b) reconstructed scPDSI over West Africa or WSDA (spanning 1500–2018 CE). (c-e) EOF

14

258 time series: WSDA is the gray line and red is instrumental scPDSI. The NRI Sahel rainfall index

259 is superimposed on the PC1 of WSDA in blue and the JISAO Sahel index in yellow. The Gulf

260 of Guinea index is also superimposed on the PC3 of WSDA in blue. PC1 of WSDA is correlated

261 to PC1 of instrumental scPDSI at R=0.77, the Sahel rainfall index from Nicholson et al. 2018

262 at R=0.66 and the JISAO Rainfall index at R=0.61. If an 11-year running mean is applied, R

263 goes up to 0.86, 0.92 and 0.91 respectively.

264

265 they are evident on both interannual and interdecadal time scales and in the historical record

266 of past centuries. EOF3 is a zonal dipole that explains 6% of the total variance and has been

267 related to a recently observed long term intensification of the Saharan heat low (Lavaysse et

268 al 2015) and enhancing effects from anthropogenic global warming (James et al 2013).

269 The EOFs of the reconstructed scPDSI (figure 3(b)) match their instrumental counterparts

270 (figure 3(a)), although EOF2 and EOF3 switch precedence, which is unsurprising considering

271 the fact that the WSDA spans a much longer period of time (519 years, 1500-2018 CE) relative

272 to the instrumental record (120 years, 1901-2020). Indeed, computing the EOFs from 1901-

273 1989, which is a period where the WSDA encompasses tree-ring only data, yields identical

274 loading patterns and are ordered in the same way (figure S2). Further, we correlate the PCs

275 of the WSDA to the corresponding PCs of instrumental scPDSI and rainfall indices from JISAO

276 and NRI over their respective overlapping time periods (figures 3 (c)-(e)). Except for the NRI

277 Gulf of Guinea index, all the other indices are significantly correlated to both the dominant

278 monopole mode of variability (EOF1) and the dipole mode (EOF3 in WSDA) that distinguishes

279 the hydrological conditions over the Sahel from the Gulf of Guinea. The NRI Gulf of Guinea

280   index is only significantly correlated to EOF3 (Table S1). This is quite intriguing, especially

281   given the absence of local tree-ring chronologies in the WSDA.

282   **4. Conclusions**

283   The West Sub-Saharan Drought Atlas (WSDA) is a new paleoclimatic reconstruction of

284   drought and wetness that reproduces several aspects of the spatio-temporal hydroclimatic

285   variability over West Africa. It is a one-half degree gridded reconstruction of summer scPDSI

286   from 1500–2018 CE and is made possible by the teleconnected climate relationship between

287   West Africa and the Mediterranean region. An ensemble version of the point-by-point

288   regression (EPPR) was used to produce the WSDA.

289   The reconstructed scPDSI of the WSDA accurately reproduced the three leading modes of

290   hydroclimate variability in West Africa and demonstrated strong skill when compared to

291   regional instrumental precipitation and drought indices. The inclusion of local tree-ring

292   chronologies in the WSDA is planned for the future and promises to yield a more robust

293   reconstruction, with a much more complete and local understanding of hydroclimatic

294   variability in West Africa. This is evident in figure S3 which shows the correlation of summer

295   (JJA) rainfall index over the Sahel with Mediterranean SST. The correlation between the

296   detrended rainfall index and SST in the Mediterranean is strong (figure S3(a)) but weakens

297   significantly when the rainfall index is first differenced (figure S3(b)). The rainfall data in

298   figure S3(a) was detrended by removing its linear best fit, which reduces the interannual

299   variability at any given location and in this case transforms the data to an overall decadal

300   variation. While differencing has the effect of removing trend and multi-year variability in a

301   data series, it also results in one fewer observation than the original series (figure S3(b)). This

302 seems to suggest the WSDA in its current form fails to retain all hydroclimatic information,

303 especially on the interannual timescale, making a strong case for the inclusion of local tree

304 ring chronologies. We also recognize the potential role modes of climate variability and remote

305 SST patterns can play in modulating the timescale of the teleconnection response in

306 Mediterranean trees, which warrants further studies.

307 It was widely believed that usual tree-ring dating methods may not be suitable for trees that

308 grow in Africa because they do not necessarily grow annual rings, but that is no longer the

309 general viewpoint today. Several researchers including Hummel 1946, Lowe 1961, Mariaux

310 1981, Detienne 1989, Jacoby 1989, Buckley et al 1995 and D'Arrigo et al 1997 have provided

311 evidence that annual rings form in several tropical species. In West Africa, some success in

312 producing annual tree-ring chronologies has also been recently reported from the Ivory Coast

313 (Ridder et al 2013) and the Cameroons (Battipaglia et al 2015). But several factors, including

314 the difficulty in identifying and interpreting growth bands, the lack of precedents

315 demonstrating successful cross dating, political instability, economic and logistical difficulties

316 have contributed to stifling further investigations of these promising results. The situation is

317 further exacerbated by the fact that most practitioners of dendrochronology are from the mid-

318 latitudes and have limited time and resources for devoting effort to evaluating tropical trees

319 for dendrochronological research (Tarhule and Hughes 2002). However, the limited success

320 in African dendrochronology reported to date suggests that the potential is there to develop

321 long tree-ring chronologies.

322

323

Acknowledgements

5. References

1. Allen D M 1971 Mean square error of prediction as a criterion for selecting variables. Technometrics 13 469–475.

2. Anchukaitis K J 2017 Tree rings reveal climate change past, present, and future Proc. Am. Philos. Soc. 161 pp. 244–263.

3. Barichivich J, Osborn T J, Harris I, van der Schrier G and Jones P D 2018 Drought [in "State of the Climate in 2018"]. Bull. Amer. Meteor. Soc. 100 S1–S306.

4. Battipaglia G, Zalloni E, Castaldi S, Marzaioli F, Cazzolla-Gatti R, Lasserre B, Tognetti R, Marchetti M and Valentini R 2015 Long Tree-Ring Chronologies Provide Evidence of Recent Tree Growth Decrease in a Central African Tropical Forest. PLOS ONE.

5. Biasutti M 2013 Forced Sahel rainfall trends in the CMIP5 archive. Journal of Geophysical Research. 118(4) 1613–1623.

6. Biasutti M, Sobel A H and Camargo S J 2009 The role of the Sahara low in summertime Sahel rainfall variability and change in the CMIP3 models. J. Clim. 22 5755–5771.

7. Buckley B, Barbetti M, Watanasak M, D'Arrigo R, Boon-chirdchoo S and Sarutanon S 1995 Preliminary dendrochronological investigations in Thailand. IAWA Bulletin 16 393–409.

8. Buckley B M, Anchukaitis K J, Penny D, Fletcher R, Cook E R, Sano M, Nam C, Wichienkeeo A, Minh T T, Hong T M 2010 Climate as a contributing factor in the demise of Angkor, Cambodia. Proc. Natl. Acad. Sci. 107 6748–6752.

9. Challinor A, Wheeler T, Garforth C, Craufurd P and Kassam A 2007 Assessing the vulnerability of food crop systems in Africa to climate change. Clim. Change 83 381–399.

359   10. Cook E R, Anchukaitis K J, Buckley B M, D'Arrigo R D, Jacoby G C and Wright W E 2010a
360   Asian Monsoon Failure and Megadrought During the Last Millennium. Science 328 (5977)
361   486–489.
362

363   11. Cook E R and Kairiukstis L A 1990 Methods of Dendrochronology. Applications in the
364   Environmental Sciences. International Institute for Applied Systems Analysis. Kluwer
365   Academic Publishers, Dordrecht, 394 p.
366

367   12. Cook E R, Meko D M, Stahle D W and Cleaveland M K 1999 Drought reconstructions for
368   the continental United States. J. Clim. 12(4) 1145–1162.
369

370   13. Cook E R, Seager R, Heim Jr R R, Vose R S, Herweijer C and Woodhouse C 2010b
371   Megadroughts in North America: placing IPCC projections of hydroclimatic change in a
372   long-term palaeoclimate context. J. Quaternary Sci. Vol. 25 pp. 48–61.
373

374   14. Cook E R, Solomina O, Matskovsky V. et al 2020 The European Russia Drought Atlas
375   (1400–2016 CE). Clim. Dyn. 54 2317–2335.
376

377   15. Cook E R, Seager R, Kushnir J, Briffa K R, Buentgen U, Frank D, Krusic P J, Tegel W, van
378   der Schrier G, Andreu-Hayles L, Baillie M, Baitttinger C, Bleicher N, Bonde N, Brown D,
379   Carrer M, Cooper R, Cufar K, Dittmar C, Esper J, Griggs C, Gunnarson B, Gunther B,
380   Gutierrez E, Haneca K, Helema S, Herzig F, Heussner K-U, Hofmann J, Janda J, Kontic R,
381   Kose N, Kyncl T, Levanic T, Linderholm H, Manning S, Melvin T, Miles D, Neuwirth B,
382   Nicolussi K, Nola P, Panayotov M, Popa I, Rothe A, Seftigen K, Seim A, Svarva H, Svoboda
383   M, Thun T, Timonen M, Touchan R, Trotsiuk V, Trouet V, Walder F, Wazny T, Wilson R
384   and Zang C 2015 Old world megadroughts and pluvials during the Common Era. Sci. Adv.
385   1(10) e1500561.
386

387   16. D'Arrigo R, Barbetti M, Watanasak M, Buckley B, Krusic P, Boonchirdchoo S and Sarutanon
388   S 1997 Progress in dendroclimatic studies of mountain pine in northern Thailand. IAWA
389   Bulletin 18 433–444.
390

391   17. Diatta S, Diedhiou C W, Dione D M, Sambou S 2020 Spatial Variation and Trend of
392   Extreme Precipitation in West Africa and Teleconnections with Remote Indices.
393   Atmosphere 11(9) 999.
394

395   18. Detienne P 1989 Appearance and periodicity of growth rings in some tropical woods. IAWA
396   Bulletin 10(2) 123–132
397

398   19. Eshun M E & Amoako-Tuffour J 2016 A review of the trends in Ghana's power sector.
399   Energy, Sustainability and Society, 6(9).
400

401   20. Fontaine B, Garcia-Serrano J, Roucou P. et al 2010 Impacts of warm and cold situations in
402   the Mediterranean basins on the West African monsoon: observed connection patterns
403   (1979–2006) and climate simulations. Clim. Dyn. 35 95–114
404

405 21. Gaetani M, Fontaine B, Roucou P & Baldi M 2010 Influence of the Mediterranean Sea on
406   the West African monsoon: intraseasonal variability in numerical simulations. J. Geophys.
407   Res., 115 D24115.

409 22. Grist J P and Nicholson S E 2001 A study of the dynamic factors influencing the variability
410   of rainfall in the West African Sahel. J. Clim. 14 1337–1359.

412 23. Haywood A M, Valdes P J, Aze T. et al 2019 What can Palaeoclimate Modelling do for you?
413   Earth Syst Environ 3 1–18.

415 24. Henderson, Gideon & Collins, Matt & Hall, Ian & Lockwood, Mike & Pälike, Heiko &
416   Rickaby, R.E.M. & Schmidt, Gavin & Turney, Chris & Wolff, Eric. 2009 Improving Future
417   Climate Prediction using Palaeoclimate Data (an outcome of The Leverhulme Climate
418   Symposium 2008 – Earth's Climate: Past, Present and Future).

420 25. Hummel F C 1946 The formation of growth rings in Entandrophragma rnacrophyllurn and
421   Khaya grandifolia. Empire Forestry Review 25 1.

423 26. Jacoby G C 1989 Overview of tree ring analysis in tropical regions. IAWA Bulletin 10(2)
424   99–108.

426 27. James R, Washington R and Rowell D P 2013 Implications of global warming for the
427   climate of African rainforests. Phil. Trans. R. Soc. B 368, 20120298.

429 28. Jung T, Ferranti L & Tompkins A M 2006 Response to the summer of 2003 Mediterranean
430   SST anomalies over Europe and Africa. J. Clim. 19 5439-5454.

432 29. LaMarche V C and Fritts H 1971 Tree Rings, Glacial Advance, And Climate In The Alps.
433   Zeitschrift Fur Gletscherkunde Und Glazialgeologie VII.

435 30. Lavaysse C 2015 Warming trends: Saharan desert warming. Nat. Clim. Change 5(9) 807–
436   808

438 31. Lorenz E N, 1956 Empirical orthogonal functions and statistical weather prediction.
439   Statistical Forecasting Project Report 1, MIT Department of Meteorology p 49.

441 32. Mariaux A 1981 Past efforts in measuring age and annual growth in tropical trees. In Age
442   and growth rate of tropical trees: new directions for research, edited by E H. Borman, and
443   G. Berlyn, 20–30. Yale University School of Forestry and Environmental Studies, Bulletin
444   94.

446 33. Meko D M 1997 Dendroclimatic reconstruction with time varying predictor subsets of tree
447   indices. J. Clim. 10 687–696.

449 34. Michaelsen J 1987 Cross validation in statistical climate forecast models. Journal of
450   Climate and Applied Meteorology 26 1589–1600.

451

35. Nicholson S E 2013 "The West African Sahel: A Review of Recent Studies on the Rainfall Regime and Its Interannual Variability", International Scholarly Research Notices, vol. 2013, Article ID 453521, **32 pages.**

36. Nicholson S E, Fink A H, Funk C 2018 Assessing recovery and change in West Africa's rainfall regime from a 161-year record. Int J Climatol 2018:1–17.

37. Peyrille P & Lafore J P 2007 An idealized two-dimensional framework to study the West African monsoon. Part II: Large-scale advection and the diurnal cycle. J. Atmos. Sci. 64 2783–2803.

38. Quan N T 1988 The prediction sum of squares as a general measure for regression diagnostics. J. Bus. Econ. Stat. 6 501–504.

39. Rayner N A. et al 2003 Global analyses of sea surface temperature, sea ice, and night marine air temperature since the late nineteenth century. J. Geophys. Res. Atmos. 108.

40. Ridder M D, Trouet V, Van den Bulcke J, Hubau W, Van Acker J and Beeckman H 2013 A tree-ring based comparison of Terminalia superba climate–growth relationships in West and Central Africa. Trees, DOI 10.1007/s00468-013-0871-3.

41. Rodwell M and Hoskins B 2001 Subtropical Anticyclones and Summer Monsoons. J. Clim. 14 3192–3211.

42. Rowell D P 2003 The impact of Mediterranean SSTs on the Sahelian rainfall season. J. Clim. 16 849–862.

43. Roudier P, Sultan S, Quirion P and Berg A 2011 The impact of future climate change on West African crop yields: what does the recent literature say? Glob. Environ. Change 21 1073–1083.

44. Salzmann U 1996 Holocene vegetation history of the Sahelian zone of NE-Nigeria: preliminary results. Paleoecology of Africa and the surrounding islands. 24 103–114.

45. Stanzel P, Kling H and Bauer H 2018 Climate change impact on West African rivers under an ensemble of CORDEX climate projections. Climate Services. 11 36-48.

46. Street-Perrott E A, Holmes J A, Waller M P, Allen M J, Barber N G H, Fothergill P A, Harkness D D, Ivanovich M, Kroon D and Perrott R A 2000 Drought and dust deposition in the West African Sahel: a 5500-year record from Kajemarum Oasis, northeastern Nigeria. The Holocene 10(3) 293–302.

47. St. George S 2014 An Overview of Tree-Ring Width Records across the Northern Hemisphere. Quaternary Science Reviews 95 132–50.

496

497   48. St. George S and Ault T R 2014 The Imprint of Climate within Northern Hemisphere Trees.
498   Quaternary Science Reviews 89 1–4.
499

500   49. St. George S, Meko D M and Cook E R 2010 The Seasonality of Precipitation Signals
501   Embedded within the North American Drought Atlas. The Holocene 20 983–88
502

503   50. Tarhule A, Hughes M K 2002 Tree-ring research in semiarid west Africa: Need and
504   potential. Tree-Ring Research 58(1/2) 31–46.
505

506   51. Touchan R, Anchukaitis K J, Shishov V V, Sivrikaya F, Attieh J, Ketmen M, Stephan J,
507   Mitsopoulos I, Christou A and Meko D M 2014 Spatial Patterns of Eastern Mediterranean
508   Climate Influence on Tree Growth. The Holocene 24 381–92.
509

510   52. Turco M, Palazzi E J and von Hardenberg, Provenzale A 2015 Observed climate change
511   hotspots. Geophys. Res. Lett. 42 3521–3528. doi: 10.1002/2015GL063891
512

513   53. van der Schrier G, Barichivich J, Briffa K R, and Jones P D 2013 A scPDSI-based global
514   data set of dry and wet spells for 1901–2009. J. Geophys. Res. Atmos. 118.
515

516   54. Waller M and Salzmann U 1999 Holocene vegetation changes in the Sahelian zone of NE
517   - Nigeria: The detection of anthropogenic activity. Paleoecology of Africa and the
518   surrounding islands. 26 85–102.
519

520   55. Wells N, Goddard S and Hayes M J 2004 A self-calibrating Palmer drought severity index,
521   J. Clim. 17 2335–2351.